Vibration of a 45° Right Triangular Cantilever Plate by a Gridwork Method

R. M. CHRISTENSEN*
Space Technology Laboratories Inc., Redondo Beach, Calif.

A free vibration solution is given for a 45° right triangular cantilever plate. A gridwork analogy for plate bending is derived and applied to obtain the first 10 natural frequencies and mode shapes. The gridwork solution is shown to give a close comparison with the experimentally determined natural frequencies and nodal patterns for the first five modes. It also is demonstrated that this gridwork solution gives a better comparison with the experimental results than does a particular corresponding Rayleigh Ritz solution.

Nomenclature

T = kinetic energy, lb-in.
U = elastic strain energy, lb-in.
E = modulus of elasticity, psi
μ = Poisson's ratio
G = modulus of rigidity, psi
x,y,z = right-hand, rectangular coordinate system
w = lateral deflection of plate or gridwork, in.
m = lumped mass, lb-sec^2/in.
M = unit moment, lb-in./in.; total moment, lb-in.; total mass of plate, lb-sec^2/in.
V = shear force, lb
a = plate dimension, in.
c = grid spacing, in.
h = plate thickness, in.
D = $Eh^3/12(1 - \mu^2)$ = flexural rigidity of a plate, lb-in.
I = moment of inertia of beams, in.^{4}
J = polar moment of inertia of beams, in.^{4}
ω = angular frequency, rad/sec
C,K = constants

Introduction

THE problem of the vibration of thin cantilever plates is a problem of considerable practical interest and one for which the exact solution, with the thin-plate theory assumptions, would be very difficult if not impossible to obtain. However, there are available various approximate solutions for the vibration of cantilever plates. Cantilevered rectangular and skewed rectangular plates have been treated by several investigators. Barton,[1] used the Rayleigh Ritz method in the study of rectangular and skew cantilever plates. Plass, Gaines, and Newsom[2] have applied Reissner's variational principle to the study of a skew cantilever plate. The finite difference technique was employed by MacNeal[3] in conjunction with an electrical analog computer to obtain a solution for the square cantilever plate. Melosh[4] developed a special means of generating a lumped parameter stiffness matrix for a plate and applied it to the problem of the square cantilever plate. In all of the preceding investigations, no more than the first five modes of vibration were determined, and varying degrees of success were experienced upon comparison with experimental data.

Triangular cantilever plates have been studied by Anderson[5] and by Lubkin and Luke.[6] The Rayleigh Ritz method was used in both of these studies; however, Anderson used beam functions to form the assumed deflection function, whereas Lubkin and Luke used a polynomial deflection function. Anderson obtained the first two modes of certain triangular cantilever plates; however, in all of his examples, the angle between either free edge and the normal to the base was never more than 30°. Lubkin and Luke obtained the first four modes for a 45° right triangular cantilever plate, as well as the solutions for certain other triangular cantilever plate problems.

In this paper, a gridwork of beams analogy for plate bending is derived and is applied to obtain the solution for a 45° right triangular cantilever plate. The resulting solution is compared with the Rayleigh Ritz solution of Lubkin and Luke and with the experimental results of Gustafson, Stokey, and Zorowski.[7, 8] The following derivation and application are subject to the classical thin-plate theory assumptions.

Beam Gridwork Requirements

Consider a gridwork of beams of an arbitrary pattern, where the beams have no bending resistance in the plane of the grid but do have bending resistance in planes normal to that of the grid and possibly have torsional resistance. By taking definitions of unit moments and shears in the gridwork similar to those in the plate, Hrennikoff[9] has shown that a necessary condition for equivalence between the infinitesimal gridwork and the plate is that the gridwork deform according to the following moment curvature relations of plate theory:

$$M_x = -D[(\partial^2 w/\partial x^2) + \mu(\partial^2 w/\partial y^2)] \quad (1)$$

$$M_y = -D[(\partial^2 w/\partial y^2) + \mu(\partial^2 w/\partial x^2)] \quad (2)$$

$$M_{xy} = (1 - \mu)D(\partial^2 w/\partial x \partial y) \qquad M_{yx} = -M_{xy} \quad (3)$$

Also, for equivalence, the infinitesimal gridwork must be subject to the same boundary conditions as the plate. These requirements for equivalence apply whether the problem to be considered is of a static or a dynamic nature. If the problem is dynamic, however, there must be an additional requirement that the mass per unit area of the infinitesimal gridwork be the same as that of the plate.

The forementioned requirements constitute necessary and sufficient conditions for equivalence between the infinitesimal gridwork of beams and the plate. For plate problems idealized by a gridwork of finite spacing, the resulting solution would be approximate.

Gridwork Stiffness Coefficients

The stiffness coefficients are derived for a square gridwork of beams (Fig. 1). By taking $EI = Dc$ and $GJ = (1 - \mu)Dc$, relations (1–3) are satisfied by the gridwork, assuming that the beams obey the elementary theories of bending and

Received by IAS August 17, 1962; revision received May 13, 1963. This paper is part of the doctoral dissertation presented by the author to Yale University in 1961. The author wishes to express his appreciation to Dana Young for his valuable advice. He also wishes to thank Vernon Neubert and Lester Chen of the Electric Boat Division of General Dynamics for allowing him the use of their computational facilities.

* Member of the Technical Staff.

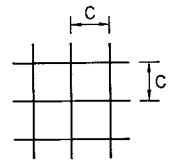

Fig. 1 Gridwork.

torsion and neglecting the Poisson's ratio effect in bending. The Poisson's ratio effect in bending is incorporated into the gridwork in the process of evaluating the corresponding stiffness coefficients.

The term "stiffness coefficients" is used to designate the forces and moments required at the nodes of the gridwork such that a particular node undergoes either a unit displacement or rotation while the displacements and rotations at all other nodes are zero. Considering a single cell of the gridwork, the stiffness coefficients for a unit displacement and a unit rotation at a node are as shown in Fig. 2. The nine stiffness coefficients M_1, $\bar{M}_1$, V_1, M_2, $\bar{M}_2$, V_2, M_3, $\bar{M}_3$, and V_3 represent the most general distribution of stiffness coefficients which could be caused by the Poisson's ratio effect in bending. That is, all beams that have a point of contact with an orthogonal beam undergoing deformation are assigned undetermined shears and moments that are designated as the Poisson's ratio effect stiffness coefficients. These nine unknown stiffness coefficients are assumed to be a linear function of some measure of bending moment $f(M)$ in the deformed orthogonal beams. This assumption is stating effectively that the Poisson's ratio effect bending moments to prevent lateral curvature are related linearly to the bending moments in the orthogonal coordinate direction, which is completely consistent with plate theory. The nine stiffness coefficients, with this assumption, can be written as

$$M_1 = c_1 f_1(M) \qquad \bar{M}_1 = c_2 f_1(M) \qquad V_1 = c_3 f_1(M) \tag{4}$$

$$M_2 = c_1 f_2(M) \qquad \bar{M}_2 = c_2 f_2(M) \qquad V_2 = c_3 f_2(M) \tag{5}$$

$$M_3 = c_1 f_3(M) \qquad \bar{M}_3 = c_2 f_3(M) \qquad V_3 = c_3 f_3(M) \tag{6}$$

where c_1, c_2, and c_3 are undetermined constants.

As an example, if the function of bending moment $f(M)$ in the deformed orthogonal beam were the bending moment at the end of the deformed beam, it is apparent from Fig. 2 that $f_1(M) = 3D/c$, $f_2(M) = 2D$, and $f_3(M) = D$. Alternatively, if the function of the bending moment were the average bending moment from the end to the midpoint of the deformed beam, it easily can be shown that $f_1(M) = \frac{3}{2}(D/c)$, $f_2(M) = \frac{5}{4}D$, and $f_3(M) = \frac{1}{4}D$. However, it is not necessary at this point to specify the function of bending moment $f(M)$ but merely to recognize its existence. It is apparent that, whatever the function $f(M)$ might be, the ratio $f_2(M)/f_3(M)$ can be designated by an undetermined nondimensional constant, say K_1. Similarly, the ratio $f_1(M)/f_3(M)$ can be taken as K_2/c, where K_2 is a nondimensional constant. It follows from (4–6) that

$$\begin{aligned} M_2/M_3 &= \bar{M}_2/\bar{M}_3 = V_2/V_3 = K_1 \\ M_1/M_3 &= \bar{M}_1/\bar{M}_3 = V_1/V_3 = K_2/c \end{aligned} \tag{7}$$

Equilibrium of the beams is provided by (8), along with (7):

$$V_3 = (M_3 + \bar{M}_3)/c \tag{8}$$

The Poisson's ratio effect condition leads to two equations. The pure bending configuration shown in Fig. 3 results from the superposition of the displacement and rotation configurations shown in Fig. 2. To satisfy the Poisson's ratio effect in bending, (9) and (10) result:

$$(2/c)\bar{M}_2 - (2/c)M_2 - \bar{M}_1 + M_1 = \mu D/c \tag{9}$$

$$-(2/c)\bar{M}_3 + (2/c)M_3 + \bar{M}_1 - M_1 = \mu D/c \tag{10}$$

Since this derivation is based on linear deformation theory, it is necessary to require that the Poisson's ratio effect stiffness coefficients satisfy the reciprocal theorem. This gives

$$M_1 = V_3 \qquad \bar{M}_1 = V_2 \qquad \bar{M}_3 = M_2 \tag{11}$$

Using (7) and (8), (11) becomes

$$\begin{aligned} (1 - K_2)M_3 + \bar{M}_3 &= 0 \\ [K_1/(K_1 - K_2)]M_3 + \bar{M}_3 &= 0 \\ -K_1 M_3 + \bar{M}_3 &= 0 \end{aligned} \tag{12}$$

The coefficients of M_3 in the three equations in (12) are identical if K_1 and K_2 satisfy (13):

$$K_1 + 1 = K_2 \tag{13}$$

The constants K_1 and K_2 are not uniquely determined and may be selected in any manner such that they satisfy (13). M_3 and $\bar{M}_3$ then are found from any one of the three equations in (12) along with either (9) or (10), which are identical for K_1 and K_2 satisfying (13). V_3 follows from (8), and the other six stiffness coefficients follow from (7). The nine Poisson's ratio effect stiffness coefficients, in terms of K_2, are shown in Table 1.

Theoretically, any value of K_2 other than 2, as noted from Table 1, gives exact equivalence of the infinitesimal gridwork and the plate. However, it is reasonable to expect, for gridworks of finite spacing, that there might be an optimum value for K_2 relative to a particular solution parameter in a particular problem. Nevertheless, the usefulness of this gridwork

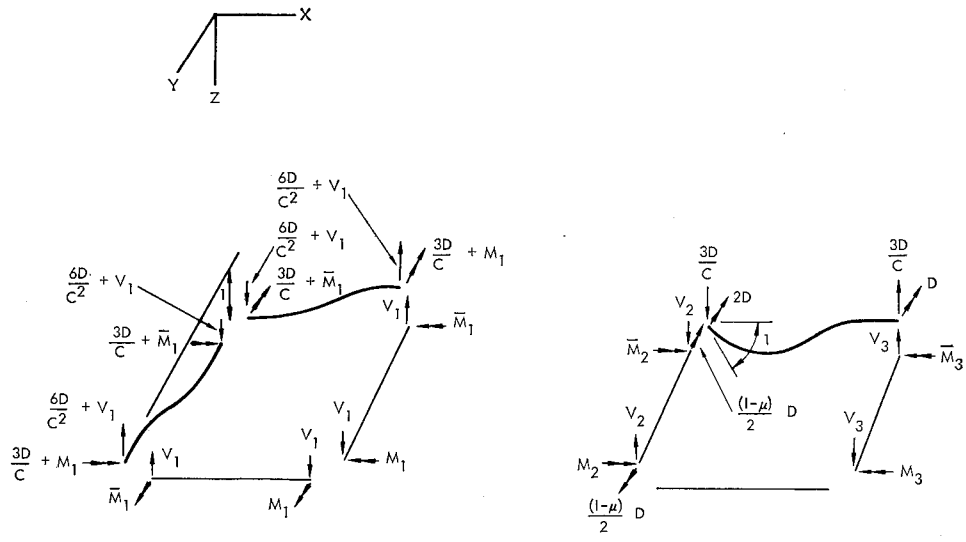

Fig. 2 Stiffness coefficients.

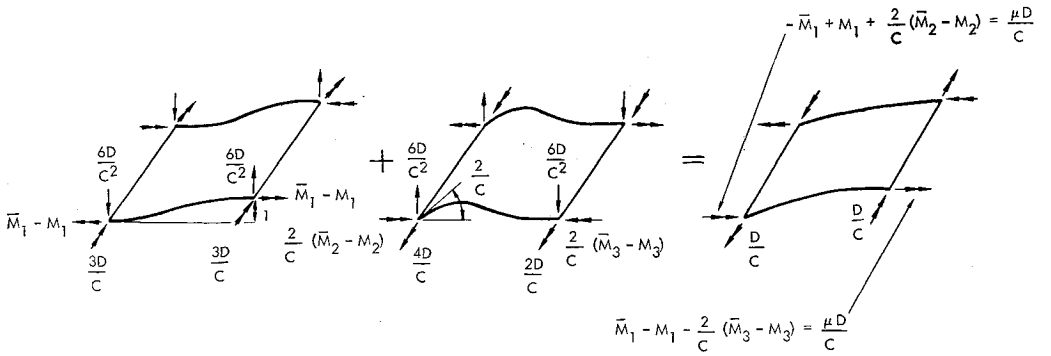

Fig. 3 Poisson's ratio effect in bending.

method of solution of plate bending problems would be in the application to problems in which there is no prior knowledge of the solution. Thus it is desirable to seek a value for K_2 which might be expected to be near this optimum value for typical plate bending problems. The method used herein to establish this value for K_2 involves the comparison of the strain energy of a plate, in a certain configuration of bending, with the strain energy of corresponding gridworks in the same configuration of bending. The bent configuration taken is that shown in Fig. 4. The sinusoidal shape is chosen for the optimization of K_2 inasmuch as it is of fundamental importance in static bending, vibration, and wave propagation in plates. The limits of integration are taken over a half wavelength in both coordinate directions since, in plate solutions involving sine waves, these appear in half wavelengths and multiples of half wavelengths.

The deflection shape given in Fig. 4 and Eq. (14), when inserted into the energy expression (15), yields the value (16):

$$w = (\Delta/2)\sin(\pi x/a)\sin(\pi y/a) \tag{14}$$

$$U_P = \frac{D}{2}\int_{-a/2}^{a/2}\int_{-a/2}^{a/2}\left[\left(\frac{\partial^2 w}{\partial x^2}\right)^2 + \left(\frac{\partial^2 w}{\partial y^2}\right)^2 + 2\mu\frac{\partial^2 w}{\partial x^2}\frac{\partial^2 w}{\partial y^2} + 2(1-\mu)\left(\frac{\partial^2 w}{\partial x \partial y}\right)^2\right]dxdy \tag{15}$$

$$U_P = 12.18(\Delta^2 D/a^2) \tag{16}$$

The strain energy of the three gridworks shown in Fig. 5 is found from

$$U_G = \tfrac{1}{2}\bar{\delta}S\delta \tag{17}$$

where $\bar{\delta}$ and δ are the row and column matrices, respectively, of rotations and displacements at the nodes of the gridworks, and S is the stiffness matrix of the gridworks. The stiffness matrix S for the three gridworks is built up from the stiffness coefficients shown in Fig. 2 and Table 1. The rotations and displacements at the nodes of the gridworks are taken to be equal to those at the corresponding points on the plate.

The strain energy determined in the manner just described for the three gridworks shown in Fig. 5 is found to be

$$U_{1G} = (\Delta^2 D/8a^2)\{8\pi^2(10 + 2^{1/2}) - 384\,(2)^{1/2}\pi + 1536\,(2 - 2^{1/2}) + [\mu/(K_2 - 2)^2]\times[8[96 - 64\,(2)^{1/2} - 2\pi^2 + \pi^2\,2^{1/2}]K_2^2 + 32\,\pi[4 + 2\pi - 4\,(2)^{1/2} - 2^{1/2}\,\pi]K_2 + 16\pi^2[2\,(2)^{1/2} - 3]]\} \tag{18}$$

Table 1 Poisson's ratio effect stiffness coefficients

Subscript	3	2	1	
M	1	$K_2 - 1$	K_2/c	$\times\dfrac{\mu D}{(K_2-2)^2}$
$\bar{M}$	$K_2 - 1$	$(K_2-1)^2$	$K_2(K_2-1)/c$	
V	K_2/c	$K_2(K_2-1)/c$	K_2^2/c^2	

$$U_{2G} = (\Delta^2 D/16a^2)\{9(11\pi^2 - 36\pi\,3^{1/2} + 108) + [\mu/(K_2-2)^2][9(9-\pi^2)K_2^2 + 18\pi[2\pi - 3(3)^{1/2}]K_2 - 9\pi^2]\} \tag{19}$$

$$U_{3G} = (\Delta^2 D/2a^2)\{(5\pi^2 - 24\pi + 48) + [\mu/(K_2-2)^2]\times[(8-\pi^2)K_2^2 + 4\pi(\pi-2)K_2 - 2\pi^2]\} \tag{20}$$

These three expressions for strain energy can be written symbolically in the form

$$U_G = U_I + U_{PR} \tag{21}$$

U_I does not involve explicitly either Poisson's ratio or K_2. U_{PR}, here called the Poisson's ratio energy, involves both Poisson's ratio as a coefficient and K_2, in quadratic form, as

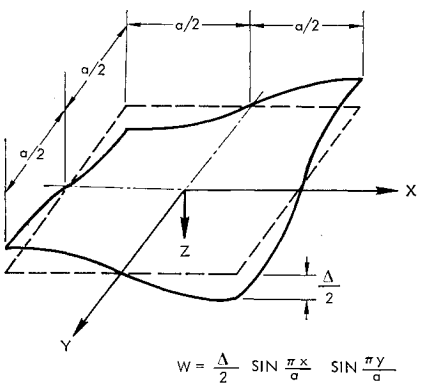

Fig. 4 Plate element.

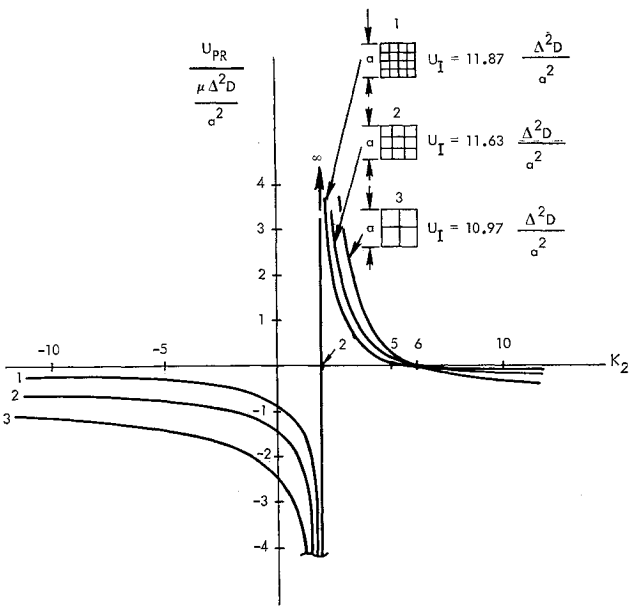

Fig. 5 Poisson's ratio energy.

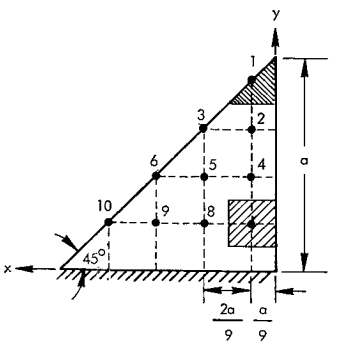

Fig. 6 45° right triangular cantilever plate.

a factor in the numerator and the denominator. U_{PR} is recognized to involve energy contributions from both the torsion of the beams and the Poisson's ratio effect in bending. U_{PR} vs K_2, for the three gridworks taken, is plotted in Fig. 5. Since, from (16), the Poisson's ratio energy in the plate element is zero, it is considered desirable that the Poisson's ratio energy in the gridworks, U_{PR}, be as near to zero as possible. As seen from Fig. 5, the value $K_2 = 6$ very nearly gives $U_{PR} = 0$ for all three gridworks. On this basis, $K_2 = 6$ is considered to be the most reasonable value to use in subsequent applications, although it should be emphasized that any value of K_2 would provide convergence to the exact solution as the grid spacing is made infinitesimal.

It is interesting to note that the value $K_2 = 6$ corresponds to the previously discussed function of bending moment $f(M)$ being taken as the average bending moment from the ends to the midpoints of the deformed beams. This measure of moment is compatible directly with the manner of the lumping of the plate flexural rigidity D into the beam EI. Also, it should be noted that, although $K_2 = 6$ corresponds to nearly zero Poisson's ratio energy for the gridworks deformed sinusoidally, this term would not be expected to vanish for a general deformation shape.

45° Right Triangular Cantilever Plate

The 45° right triangular cantilever plate is idealized by the gridwork shown in Fig. 6. In effect, the skewed edge of the plate is idealized as a stepped edge compatible with the square grid. Convergence to the exact solution, as the grid spacing is made infinitesimal, is not invalidated by this idealization. Ordinarily, the total mass of the plate would be lumped directly as the nodes of the gridwork; however, this procedure has the objectionable feature that, for the higher modes, the concentration of the mass gives an unrealistically large value for the kinetic energy, causing the natural frequencies to be too low. This difficulty can be overcome by placing weighted inertia terms at the nodes. Referring to Fig. 7a, illustrating the one-dimensional case rather than simply lumping the mass between $x = \pm(c/2)$ at node n, the inertia term that is to be concentrated at n is taken as the integrated distributed inertia between $x = \pm(c/2)$. This procedure is similar to that described by Bisplinghoff et al.[10] in obtaining a "weighting matrix" for effectively replacing distributed static and inertia forces by concentrated forces through the use of standard integration formulas such as Simpson's rule. A special formula for the weighted inertia terms will be derived here for reasons described following its derivation.

The expression for the deflection shape in Fig. 7a is taken as

$$w = b_1 + b_2\,(x/c) + b_3 \cos\pi\,(x/c)\left|\cos\pi\,(x/c)\right| \qquad (22)$$

where b_1, b_2, and b_3 are constants that are determined in terms of w_{n-1}, w_n, and w_{n+1}. Using this deflection expression, the integration shown in (23) can be performed:

$$\int_{-c/2}^{c/2} w\,dx = \frac{c}{8}\,(w_{n-1} + 6w_n + w_{n+1}) \qquad (23)$$

The inertia term that is to be lumped at node n in Fig. 7a is then

$$F = \gamma\omega^2(c/8)(w_{n-1} + 6w_n + w_{n+1}) \qquad (24)$$

where γ is the mass per unit length. The reason for the selection of (22) as the deflection shape now will be made clear. The first two terms in (22) are necessary to allow a translation and rotation of the three nodes in Fig. 7a. The third term in (22) is included so that the kinetic energy of a lumped system of infinite extent in the highest mode of vibration, with adjacent nodes having displacements of the same amplitude but opposite sign, is exactly the same as that of the distributed mass system with the same wavelength. Specifically, it easily is shown that the maximum kinetic energy per node associated with the highest mode of vibration, of amplitude A, for direct mass lumping gives $T = \gamma c\omega^2A^2/2$, whereas that determined using (24) gives $T = \gamma c\omega^2A^2/4$. The comparable kinetic energy for the distributed mass system with sinusoidal waves is $T = \gamma c\omega^2A^2/4$. Thus, the kinetic energy of a lumped system using inertia terms specified by (24) converges to the exact value of the kinetic energy for the highest mode, whereas the direct mass lumping technique converges to twice the exact value.

The deflection expression (22) can be used to obtain weighted inertia terms appropriate to node n in Fig. 7b. Following the same procedure used to obtain (23), it is found that

$$\int_{-c/2}^{c/2} w\,dx = \frac{c}{8}\,[7\,w_n + 2\,w_{n+1} - w_{n+2}] \qquad (25)$$

$$\int_{0}^{c/2} w\,dx = \frac{c}{8}\,[3w_n + w_{n+1}] \qquad (26)$$

There undoubtedly are deflection expressions other than (22) which could be employed successfully to the same purpose just outlined, although the application of (22) appears to be especially simple and direct. The usage of (22) for replacing distributed inertia terms by lumped inertia terms is designed specifically to improve the kinetic energy formulation for the higher frequency modes of the lumped system over that given by direct mass lumping. There is no assurance that the usage of (22) improves the kinetic energy formulation for the lower frequency modes. However, inasmuch as the lower modes naturally would be insensitive compared with the higher modes to the particular means of mass or inertia term lumping, it is reasonable to focus attention on the improvement of the higher mode kinetic energy

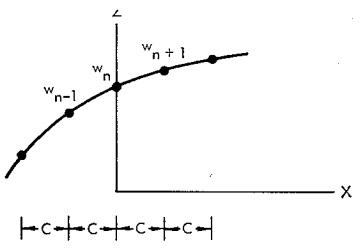

Fig. 7 Deflection shape.

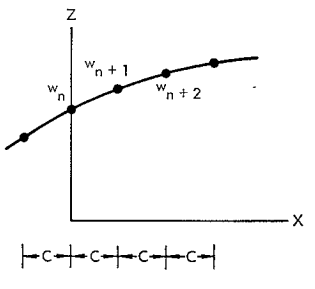

Table 2 Transverse inertia terms

Node

$$
\begin{array}{c}
1 \\ 2 \\ 3 \\ 4 \\ 5 \\ 6 \\ 7 \\ 8 \\ 9 \\ 10
\end{array}
\begin{bmatrix}
6 & 2 & & & & & & & & \\
1 & 14 & & 1 & & & & & & \\
 & 1 & 6 & & 1 & & & & & \\
 & 1 & & 13 & 2 & -1 & 1 & & & \\
 & & 1 & 1 & 12 & 1 & & 1 & & \\
 & & & & 1 & 6 & & & 1 & \\
 & & & 1 & & & 13 & 2 & -1 & \\
 & & & & 1 & & 1 & 12 & 1 & \\
 & & & & & 1 & & 1 & 12 & 1 \\
 & & & & & & & & 1 & 6
\end{bmatrix}
\times
\begin{Bmatrix} w_1 \\ w_2 \\ w_3 \\ w_4 \\ w_5 \\ w_6 \\ w_7 \\ w_8 \\ w_9 \\ w_{10} \end{Bmatrix}
\times \left(-\frac{M\omega^2}{162} \right)
$$

Table 3 Frequencies and amplitude ratios

Mode	1[a]	2	3	4	5	6	7	8	9	10
Experimental freq. $\times (D/Ma^2)^{1/2}$, Ref. 7	4.17	16.4	23.0	39.3	53.3	69.9	...	...	...	...
Gridwork freq. $\times (D/Ma^2)^{1/2}$	4.35	16.76	23.01	38.90	53.65	60.32	78.26	90.92	107.1	148.6
Rayleigh Ritz freq. $\times (D/Ma^2)^{1/2}$, Ref. 6	4.42	16.9	23.7	43.5	...	...	...	...	...	...
Gridwork displacement amplitude ratios										
Node 1	1	1	1	1	1	1	1	1	1	1
Node 2	0.65	0.29	−0.27	0.07	−0.74	−1.01	−1.15	−1.02	−1.32	−1.60
Node 3	0.56	−0.94	0.45	−3.62	−0.18	1.39	1.86	−1.03	1.64	3.70
Node 4	0.33	−0.05	−0.81	0.39	−0.06	0.04	1.36	1.10	2.32	5.08
Node 5	0.28	−0.78	−0.07	−0.31	0.40	−0.002	−2.08	1.74	−1.65	−6.98
Node 6	0.20	−1.33	0.43	1.88	0.03	−1.99	4.38	−0.37	−0.65	5.54
Node 7	0.10	−0.05	−0.47	0.44	0.55	0.90	3.05	−1.66	−1.05	−5.48
Node 8	0.08	−0.32	−0.11	0.49	0.47	0.27	−3.77	−0.70	−0.43	8.62
Node 9	0.06	−0.45	0.12	1.24	−0.19	0.27	−1.92	−1.17	2.76	−6.00
Node 10	0.02	−0.31	0.14	1.78	−1.28	2.65	0.84	1.18	−1.99	2.89

[a] Units are given in radians per second.

formulation. Of course, the final evaluation of the usefulness of any particular inertia term lumping procedure rests on the comparison of data so obtained with experimental or other analytical data. Such a comparison will be made in the following.

The inertia terms for the gridwork in Fig. 6 are obtained using (23, 25, and 26). The transverse inertia terms thus obtained are as shown in Table 2.

The gridwork analogy of the previous section, with $K_2 = 6$ and $\mu = 0.3$, is used to construct the associated 30×30 stiffness matrix of the gridwork in Fig. 6. Each node is allowed rotation about axes parallel to the x and y axes and a displacement normal to the plane of the grid. The nodes at the clamped edge are restrained completely against rotations and displacements. Using this stiffness matrix and the mass matrix, which includes the inertia terms shown in Table 2, the mathematical formulation of the dynamical equations is put in the form of the standard eigenvalue problem. This has been solved on an electronic digital computer.

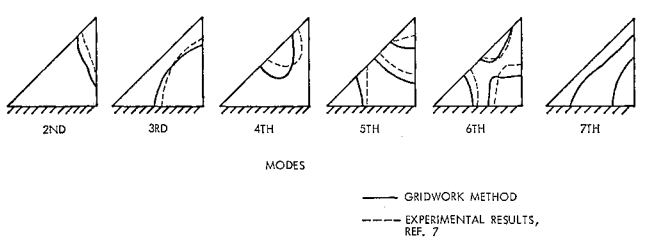

Fig. 8 Mode shapes.

The gridwork solution for the first 10 frequencies, with the associated amplitude ratios, is given in Table 3. Also given for comparison are the experimental frequencies from Refs. 7 and 8 and the Ref. 6 frequencies found by the Rayleigh Ritz method. Since the plate used in the experimental investigation had slightly different material properties in the x and y directions, the average modulus of elasticity, $E = 28.5 \times 10^6$, and $\mu = 0.3$ are used to convert the experimental frequencies to the form given in Table 3. The gridwork nodal patterns, found by plotting the deflection shapes from the amplitude ratios, are compared with the experimental nodal patterns in Fig. 8. The gridwork nodal patterns are not plotted for the modes higher than the seventh because a finer grid would be needed to determine these nodal patterns with certainty.

The gridwork solution frequencies (Table 3) compare well with the experimental frequencies for the first five modes. The nodal patterns (Fig. 8) also give a good comparison between the gridwork solution and the experimental results for all six of the experimental modes. The difference in the gridwork solution and experimental frequencies for the sixth mode is not accountable here. However, in view of the consistency of the nodal patterns for this mode, it is thought to be likely that the discrepancy in frequencies is attributable to the reported experimental value. It should be noted from Table 3 that the gridwork solution, which has 10 unknown deflection parameters, gives a consistently better comparison with the experimental frequencies than does the Rayleigh Ritz solution,[6] which had 14 unknown deflection parameters.

It is possible, using current computer methods, to solve

much higher order systems than was considered in this example. Thus, finer gridworks can be used, thereby giving more accurate solutions with more modes. For problems not suited to a square gridwork, the gridwork analogy presented here can be extended to the rectangular case. It should be mentioned that gridwork methods can be adapted to plates of general shapes by idealizing the curved or skewed edges of the plate as stepped edges compatible with the grid pattern, as was done here with the triangular cantilever plate.

The gridwork analogy method presented in this paper will be extended, in a subsequent paper, to include the effects of shear deformation and rotatory inertia.

References

[1] Barton, M. V., "Vibration of rectangular and skew cantilever plates," J. Appl. Mech. **18**, 129–134 (1951).

[2] Plass, H. J., Jr., Gaines, J. H., and Newsom, C. D., "Application of Reissner's variational principle to cantilever plate deflection and vibration problems," J. Appl. Mech. **29**, 127–135 (1962).

[3] MacNeal, R. H., "The solution of elastic plate problems by electrical analogies," J. Appl. Mech. **18**, 59–67 (1951).

[4] Melosh, R. J., "A stiffness matrix for the analysis of thin plates in bending," J. Aerospace Sci. **28**, 34–42 (1961).

[5] Anderson, B. W., "Vibration of triangular cantilever plates by the Ritz method," J. Appl. Mech. **21**, 365–370 (1954).

[6] Lubkin, J. L. and Luke, Y. L., "Modes and frequencies of wings of triangular planform," Wright Air Dev. Center TR 56-335, pp. 1–46 (June 1956).

[7] Gustafson, P. N., Stokey, W. F., and Zorowski, C. F., "An experimental study of natural vibrations of cantilevered triangular plates," J. Aeronaut. Sci. **20**, 331–337 (1953).

[8] Gustafson, P. N., Stokey, W. F., and Zorowski, C. F., "The effect of tip removal on the natural vibrations of uniform cantilevered triangular plates," J. Aeronaut. Sci. **21**, 621–633 (1954).

[9] Hrennikoff, A., "Solution of problems of elasticity by the framework method," J. Appl. Mech. **8**, A-169–A-175 (1941).

[10] Bisplinghoff, R. L., Ashley, H., and Halfman, R. L., *Aeroelasticity* (Addison-Wesley Publishing Co. Inc., Reading, Mass., 1955), p. 30.

AUGUST 1963 AIAA JOURNAL VOL. 1, NO. 8

Flutter Analysis of Flat Rectangular Panels Based on Three-Dimensional Supersonic Potential Flow

H. J. CUNNINGHAM*
NASA Langley Research Center, Hampton, Va.

A procedure has been developed for computing flutter characteristics of single finite panels, particularly at low supersonic Mach numbers where static and quasistatic aerodynamic approximations are not valid. Air forces from exact linearized potential-flow theory are used. The panel is considered as finely divided into many boxes, and the aerodynamic influence coefficients between all pairs of boxes are computed by numerical integration. The flutter analysis is a modal type of analysis which can be used with the box method for calculation of the flutter stability of any flat or nearly flat panel, whether of isotropic or anisotropic stiffness, and even for buckled panels for which the flutter is a small-amplitude, simple harmonic, superimposed motion to which linear theory would apply. Certain results are presented for flat unstressed isotropic panels. Variables whose effects were studied are panel length-to-width ratio, Mach number, and the air cavity behind the panel. Panels with simply supported and with clamped edges were studied.

Nomenclature

a_s = speed of sound
A_φ = aerodynamic influence coefficient giving the velocity potential at a box due to unit downwash on another box [Eqs. (3) and (9)]
B_s = number of boxes in stream direction
B_{xs} = number of boxes in cross-stream direction
d = depth of cavity behind the panel
g = structural damping coefficient of the panel
h_i,h_j = distribution over the panel of mode shape for modes i and j [Eq. (14)]
$H_j(x,y,\tau)$ = distribution of time-varying vertical deflection of panel for mode j [Eq. (14)]
$i = (-1)^{1/2}$ = unit of imaginaries
I_{G1},I_{G2},I_{G3} = integrals in A_φ [Eqs. (10–12)]
$k_\epsilon = \omega\epsilon/V$ = reduced frequency with reference length ϵ
$k_l = \omega l/V$ = reduced frequency with reference length l
l = length of panel in stream direction
m_A = mass per unit of surface area of panel
$M = V/a_s$ = Mach number
M_i = generalized mass for mode i
M_i^* = M_i/lwm_A (applicable for uniform panel only)
N = number of modes in a flutter analysis
Δp_j = perturbation pressure due to mode j [Eq. (17)]
q = dynamic pressure of airstream
$q_i(\tau),q_j(\tau)$ = time-varying generalized coordinate of motion for modes i and j
$\bar{q}_j$ = complex amplitude of q_j [Eq. (14)]
Q_{ij} = generalized aerodynamic force from the pressure due to mode j and the modal deflection of mode i [Eq. (18)]
Q_{ij}^* = nondimensional computational quantity contained in Q_{ij} [Eq. (21)]
t = thickness of panel
u,v = transformed panel coordinates in x and y directions, respectively, based on $\epsilon/2$ as a reference length [Eq. (5)]
u_1,u_2,v_1,v_2 = lower and upper limits of integration with respect to u and to v [Eq. (6)]
w_j = downwash velocity at the panel surface for mode j
w = width of panel in the cross-stream direction
x,y = panel coordinates in stream and cross-stream directions, respectively (see Fig. 1), based on ϵ as a reference length in Eqs. (3) and (5)
x_m,y_n = values of x and y at center of box m,n

Presented at the IAS 31st Annual Meeting, New York, January 21–23, 1963; revision received June 10, 1963.

* Aerospace Engineer. Member AIAA.